Phase equilibria and crystal chemistry in the calcia–silica–yttria system

David L. Poerschke [a,*], Talia L. Barth [a], Olga Fabrichnaya [b], Carlos G. Levi [a]

[a] Materials Department, University of California, Santa Barbara, CA 93106-5050, United States
[b] Institute for Materials Science, Technical University Bergakademie Freiberg, 09599 Freiberg, Germany

ABSTRACT

The phase equilibria in the $CaO–SiO_2–Y_2O_3$ system have been assessed at 1400 °C and 1600 °C using powders prepared by precipitation from precursors. Four ternary phases were identified: Ca/Y-cyclosilicate ($Ca_3Y_2Si_6O_{26}$), silico-carnotite ($Ca_3Y_2Si_3O_{12}$), cuspidine (nominally $Ca_2Y_2Si_2O_9$), and apatite (solid solution based on $Ca_2Y_8Si_6O_{26}$). The melting temperature of each ternary phase was measured and the shape of the liquid field at 1600 °C was assessed. The study emphasizes understanding the extent and crystallographic origin of the solid solution homogeneity range for apatite between $Ca_{0.5}Y_9(SiO_4)_6O_2$ and $Ca_{2.5}Y_{7.5}(SiO_4)_6O_{1.75}$, deviations from the nominal cuspidine stoichiometry, and solubility of Y_2O_3 in the high-temperature α-Ca_2SiO_4 polymorph. The results are discussed in the context of molten silicate (CMAS) degradation of thermal and environmental barrier coatings (T/EBCs).

© 2016 Elsevier Ltd. All rights reserved.

1. Introduction

The degradation of thermal and environmental barrier coatings (TBCs and EBCs) by molten silicate deposits [1–5] has been identified as a fundamental barrier to the development of more efficient gas turbine engines [6]. Depending on the specific service environment, the deposits cover a range of compositions with variations in the fractions of CaO, MgO, $AlO_{1.5}$,[1] FeO_x, and other minor constituents [6]. For instance, based on analysis of ex-service components [5], many laboratory studies have used a model deposit composition $C_{33}M_9A_{13}S_{45}$[2] while others have studied deposits representative of debris sources such as volcanic ash [7], $C_6M_3F_9A_{20}S_{62}$, or desert sand [8], $C_{37}M_5F_2A_8S_{49}$. A leading mitigation strategy involves implementing coating materials (zirconates, hafnates, and/or silicates) with a high rare earth oxide ($REO_{1.5}$) concentration to promote reactivity with the molten deposits. These reactions convert the melt to an assemblage of crystalline phases, simultaneously reducing the molten volume and hindering the deleterious infiltration into the porous or segmented coating structure.

This reactive crystallization process was first observed with $Gd_2Zr_2O_7$ coatings, which rapidly form an oxyapatite phase, $Ca_2Gd_8(SiO_4)_6O_2$, as $GdO_{1.5}$ reacts with CaO and SiO_2 from the melt [6,9]. The combined volume of apatite and the $GdO_{1.5}$-depleted, ZrO_2-based fluorite phase are greater than that of the dissolved coating leading to filling of the open microstructure features with reaction products. Similar apatite-forming reactions, albeit with varying efficacy for blocking melt infiltration or coating recession, are reported for coatings containing other REs including $YbO_{1.5}$ [10,11], $YO_{1.5}$ [12–14], $SmO_{1.5}$ [15], $NdO_{1.5}$ [16], and $LaO_{1.5}$ [17].

The reaction mass balances (and ultimate CMAS mitigation efficacy) are dictated by the multi-component phase equilibria including (i) changes in the predominant silicate reaction product(s) (e.g., apatite, cuspidine [11], and/or garnet [11,14]), (ii) cation-size dependence on $REO_{1.5}$ partitioning between reaction products [18], (iii) the melt saturation limits, and (iv) the solid-solution homogeneity ranges. General trends have been extracted from model experiments involving exposure of coatings or sintered pellets to CMAS melts [18–20] However, these experiments invariably capture a combination of thermodynamic and kinetic effects. A more complete view of the underlying phase equilibria is needed to understand the relevant effects in the context of changes in melt constitution or coating material. Specifically, little is known [21] about the $CaO–SiO_2–REO_{1.5}$ systems, which capture

---

* Corresponding author.
  E-mail address: poerschke@engineering.ucsb.edu (D.L. Poerschke).

[1] For convenience in relating compositions to specific ionic substitutions, all compositions are specified in molar percentages or ratios based on single cation formula units (i.e., $AlO_{1.5}$ rather than Al_2O_3) for end member oxides. Except where necessary to understand the crystal chemistry of solution phases, the compact notation C = CaO, S = SiO_2, and Y = $YO_{1.5}$ is used, e.g., CS for $CaSiO_3$, C2S for Ca_2SiO_4, etc.

[2] Based on molar concentrations, $C_{33}M_9A_{13}S_{45}$ corresponds to 33mol% CaO–9mol% MgO–13mol% $AlO_{1.5}$–45mol% SiO_2. Literature CMAS compositions simplified to include only Si, Ca, Mg, Al, and Fe oxides.
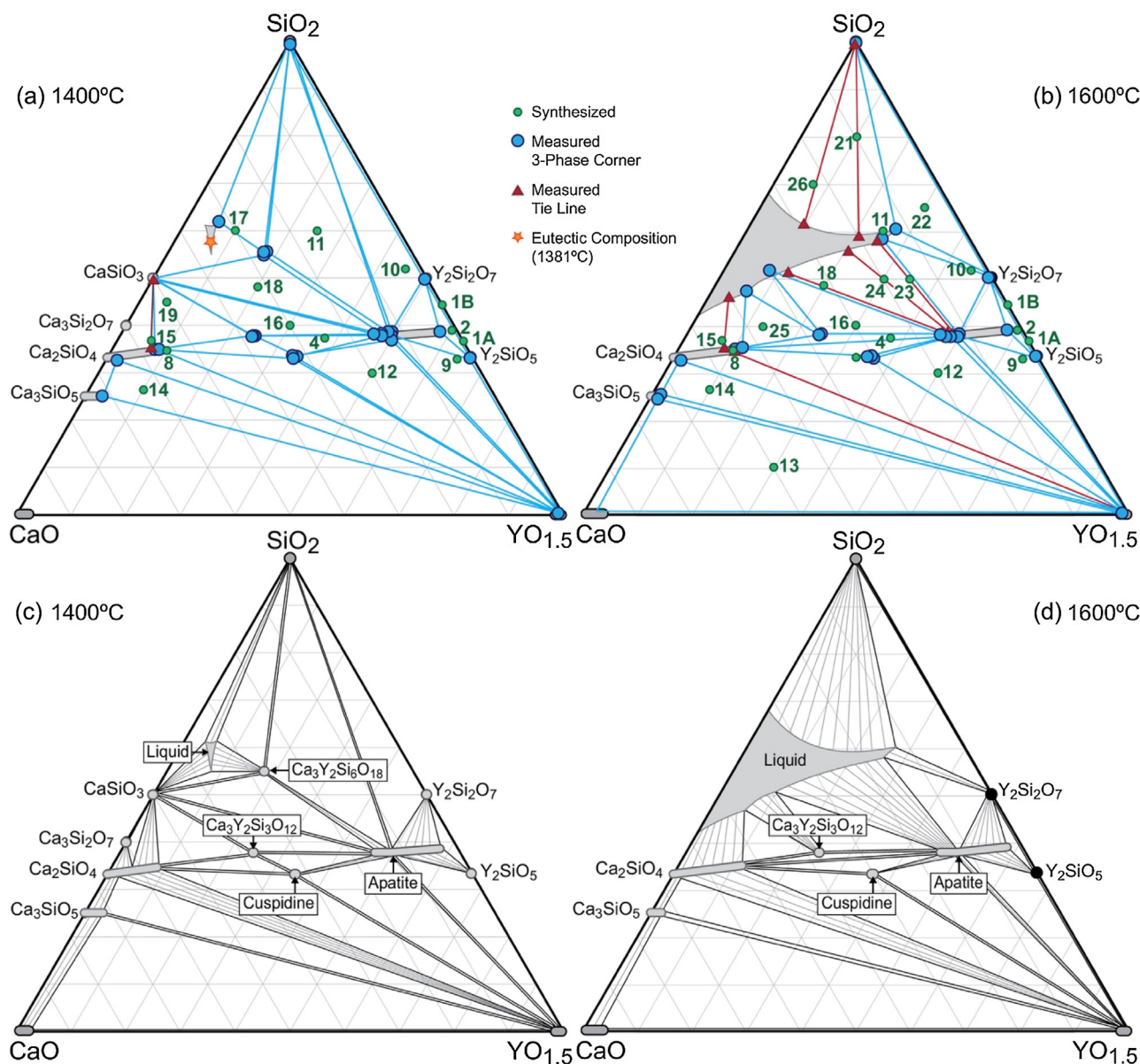
Fig. 1. CaO–SiO$_2$–YO$_{1.5}$ phase diagrams at 1400 °C and 1600 °C. The (a,b) experimentally determined three-phase triangles and tie lines based on data in Table 3 were used to construct the (c,d) complete diagrams with inferred tie lines.

the predominant CMAS deposit constituents [6] (CaO and SiO$_2$) and crystallization products such as apatite and cuspidine.

As part of a larger effort to understand the phase equilibria underpinning CMAS-T/EBC interactions, the present investigation focuses on elucidating the CaO–SiO$_2$–YO$_{1.5}$ (CSY) pseudo-ternary. This system was selected to leverage existing phase equilibria data and thermodynamic modeling of the CMAS constituents [22,23], YO$_{1.5}$ and ZrO$_2$ (as coating constituents), and combinations thereof [24–26] In addition to their importance in the T/EBC community, CSY phases are also relevant for a variety of functional applications including use as phosphor hosts [27,28] and ionic conductors [29,30]. In these applications, information about the phase relationships and homogeneity ranges is helpful to efforts to optimize the functional performance of each material.

Prior investigations have identified four ternary CSY phases [31–34] and select phase relationships [35,36]. but there has not been a systematic study of the solution phases or the effects of their homogeneity ranges on the equilibrium relationships. There is also no information about the solid-liquid phase equilibria or ternary

melting behavior. This study addresses these needs by determining the ternary CSY equilibria at 1400 °C and 1600 °C and evaluating the melting behavior for the ternary phases.

2. Background on phase equilibria

The known binary and ternary CSY phases are summarized in Table 1. Details relevant to the current investigation are provided in the following sections.

2.1. Quasibinary subsystems

The CaO–SiO$_2$ binary has been studied extensively [37] owing to its importance for understanding phases relevant to geology, cement manufacture [38], and slag chemistry [39]. There are four binary compound stoichiometries: CaSiO$_3$, Ca$_3$Si$_2$O$_7$, Ca$_2$SiO$_4$, and Ca$_3$SiO$_5$. Three CS polymorphs are reported. At 1125 °C wollastonite (β) transforms to pseudo-wollastonite (α), which melts congruently at 1544 °C. The β form consists of long [Si$_n$O$_{3n}$]$^{2n-}$